Bottomonium above Deconfinement in Lattice Nonrelativistic QCD

G. Aarts,[1] S. Kim,[2] M. P. Lombardo,[3] M. B. Oktay,[4] S. M. Ryan,[5] D. K. Sinclair,[6] and J.-I. Skullerud[7]

[1]*Department of Physics, Swansea University, Swansea SA2 8PP, United Kingdom*
[2]*Department of Physics, Sejong University, Seoul 143-747, Korea*
[3]*INFN-Laboratori Nazionali de Frascati, I-00044, Frascati (RM) Italy*
[4]*Department of Physics and Astronomy, University of Utah, Salt Lake City, Utah 84112-0830, USA*
[5]*School of Mathematics, Trinity College, Dublin 2, Ireland*
[6]*HEP Division, Argonne National Laboratory, 9700 South Cass Avenue, Argonne, Illinois 60439, USA*
[7]*Department of Mathematical Physics, National University of Ireland Maynooth, Maynooth, County Kildare, Ireland*
(Received 21 October 2010; published 11 February 2011)

We study the temperature dependence of bottomonium for temperatures in the range $0.4T_c < T < 2.1T_c$, using nonrelativistic dynamics for the bottom quark and full relativistic lattice QCD simulations for $N_f = 2$ light flavors on a highly anisotropic lattice. We find that the Υ is insensitive to the temperature in this range, while the χ_b propagators show a crossover from the exponential decay characterizing the hadronic phase to a power-law behavior consistent with nearly free dynamics at $T \simeq 2T_c$.

Introduction.—Heavy quark bound states are important probes of the dynamics in the quark-gluon plasma: charmonium suppression [1,2] has been observed at a variety of energies at SPS [3] and RHIC [4]. While the melting of bound states certainly reduces quarkonium production, the converse is not necessarily true: different, even competing, effects make it difficult to interpret charmonium suppression patterns. It has been noted that such effects should be less significant for bottomonium (see, e.g., Ref. [5] for a review). Since at LHC energies bottomonium will be produced copiously [6,7], precision studies of the suppression pattern and its unambiguous link with the spectrum of bound states should be possible. The advent of the LHC calls therefore for precision studies of bottomonium at high temperature.

Because of the large mass of the bottom quark, it is customary to study the bottomonium spectrum at zero temperature using nonrelativistic QCD (NRQCD) [8–10] and other effective field theories [11]. In this Letter, we employ NRQCD to study the response of bottomonium to a thermal medium of quarks and gluons in the temperature range $0.4T_c < T < 2.1T_c$, at the onset of the initial temperature attained in heavy ion collisions at the LHC [12]. We use dynamical anisotropic lattice configurations with two light flavors, which have been exploited before in a relativistic study of charmonium [13,14]. As explained below, the use of NRQCD is a controlled approach which avoids many of the unwanted systematic effects encountered when using relativistic dynamics for bottomonium at nonzero temperature [15–17]. An early study of bottomonium at nonzero temperature using NRQCD (on a quenched background for the $^1S_0$ and $^3S_1$ channels only) can be found in the pioneering work [18].

NRQCD at nonzero temperature.—In contrast to the case at zero temperature [11], the use of potential models to analyze quarkonium at nonzero temperature is less well defined due to the uncertainty about which potential to use (see, e.g., Ref. [19] and references therein). Recently this has been clarified by casting the problem in the language of effective field theory at nonzero temperature [20–25] (see Ref. [26] for a clear introduction). The series of effective field theories that is obtained is based on hierarchies such as $M \gg T > g^2M > gT \gg g^4M$ or $M \gg g^2M > T \gg gT \gg g^4M$, where M is the heavy quark mass and g is the gauge coupling. Integrating out thermal degrees of freedom generates an imaginary part for the interquark potential, which highlights the absence of stable states once they are immersed in a thermal medium. Limitations of approaches based on potential models and the Schrödinger equation are discussed in Ref. [27].

In the effective thermal field theory setup [20–26], NRQCD is the first theory obtained when integrating out ultraviolet degrees of freedom. We study this theory nonperturbatively on the lattice and therefore do not require weak-coupling arguments as in the hierarchy of effective field theories alluded to above. Since NRQCD relies on the scale separation $M \gg T$ and we study temperatures up to $2T_c \simeq 400$ MeV, its application is fully justified.

NRQCD has an additional advantage. At nonzero temperature, spectroscopy for relativistic quarks is hindered by the periodicity of the lattice in the temporal direction and the reflection symmetry of mesonic correlators, visible in, e.g., the standard relation between a correlation function and its spectral function,

$$G(\tau) = \int_0^\infty \frac{d\omega}{\pi} \frac{\cosh[\omega(\tau - 1/2T)]}{\sinh(\omega/2T)} \rho(\omega). \quad (1)$$

Nontrivial spectral weight at small ω yields a constant τ-independent contribution to the correlator, which must be treated with care [28,29]. Moreover, it has been shown

that this contribution can interfere with meson spectroscopy [30], which has cast doubt on the status of results for the melting or survival of charmonium at high temperature [30,31].

In NRQCD these problems are not present. Writing $\omega = 2M + \omega'$ and dropping terms that are exponentially suppressed when $M \gg T$ [22], the spectral relation (1) reduces to

$$G(\tau) = \int_{-2M}^{\infty} \frac{d\omega'}{\pi} \exp(-\omega'\tau)\rho(\omega') \quad (\text{NRQCD}), \quad (2)$$

even at nonzero temperature. As a result, all problems associated with thermal boundary conditions are absent.

To study what to expect when quarks are no longer bound, consider free quarks in continuum NRQCD with energy $E_{\mathbf{p}} = \mathbf{p}^2/2M$. The correlators for the S and P waves are then of the form [22]

$$G_S(\tau) \sim \int \frac{d^3p}{(2\pi)^3} \exp(-2E_{\mathbf{p}}\tau) \sim \tau^{-3/2}, \quad (3)$$

$$G_P(\tau) \sim \int \frac{d^3p}{(2\pi)^3} \mathbf{p}^2 \exp(-2E_{\mathbf{p}}\tau) \sim \tau^{-5/2}; \quad (4)$$

i.e., they decay as a power for large Euclidean time. Of course, interactions and finite lattice spacing and volume effects are expected to modify this in the realistic case.

Lattice simulations.—Gauge configurations with two degenerate dynamical light Wilson-type quark flavors are produced on highly anisotropic lattices ($\xi \equiv a_s/a_\tau = 6$) of size $N_s^3 \times N_\tau$. A summary of the lattice data sets is given in Table I, while more details of the lattice action and parameters can be found in Refs. [13,14]. We computed NRQCD propagators on these configurations using a mean-field improved action with tree-level coefficients, which includes terms up to and including $\mathcal{O}(v^4)$, where v is the typical velocity of a bottom quark in bottomonium (see Ref. [33] for a discussion of the systematics). The quantum numbers we consider are listed in Table II and the operators used are those of Ref. [9].

An accurate determination of bottomonium spectroscopy requires careful tuning of the bare heavy quark mass m_b to satisfy NRQCD dispersion relations [9]. Since the main goal of this work is to study the finite-temperature

modification of NRQCD propagators, an approximate choice of $a_s m_b$ is made such that $m_b \simeq 5$ GeV.

Zero temperature results.—The zero temperature spectrum from our analysis is summarized in Table II. This spectrum is obtained using a combination of point and extended sources in the different channels, in order to extract both the ground state and the first excited state. Because level splittings are relatively insensitive to m_b and to avoid the difficulties in calculating the rest mass in NRQCD, we have combined $m_\Upsilon(1^3S_1) = 9460$ MeV (from the Particle Data Book [34]) with the mass splittings obtained from our results to predict the bottomonium spectrum.

As can be seen from Table II, the zero temperature spectrum is reproduced reasonably well. The hyperfine splitting between the $\eta_b(^1S_0)$ and $\Upsilon(^3S_1)$ is much smaller than the experimental value, due to the coarse spatial lattice spacing, the use of tree-level coefficients, the relatively heavy sea quarks and contributions of higher order in v^2 (see Ref. [33] for earlier calculations and discussions). In this study we are primarily interested in qualitative changes to S and P wave correlators as the temperature changes, so a precision determination is not a major concern.

S and P wave bottomonium in the plasma.—To investigate thermal effects, we focus on the S wave in the 1^{--} (vector) channel and the P waves in the 0^{++} (scalar), 1^{++} (axial-vector), and 2^{++} (tensor) channels, computed with point sources. Following the discussion above, our aim is to see a transition from exponential decay in the hadronic phase, $G(\tau) \sim \exp(-\Delta E\tau)$, characterizing bound states, to power-law decay, $G(\tau) \sim \tau^{-\gamma}$, see Eqs. (3) and (4), characterizing quasifree behavior.

In Fig. 1, standard effective masses, defined by

$$m_{\text{eff}}(\tau) = -\log[G(\tau)/G(\tau - a_\tau)], \quad (5)$$

are shown in both the vector and axial-vector channel at various temperatures. Single exponential decay should yield a τ-independent plateau. In both cases we find that at the lowest temperature, $T = 0.42T_c$, exponential behavior is visible provided one goes to late Euclidean times. Relevant for the topic of this Letter is that in the case of the

TABLE I. Summary of the lattice data set. The lattice spacing is set using the $1P - 1S$ spin-averaged splitting in charmonium [32].

N_s	N_τ	a_τ^{-1}	T (MeV)	T/T_c	Number of configurations
12	80	7.35 GeV	90	0.42	74
12	32	7.06 GeV	221	1.05	500
12	24	7.06 GeV	294	1.40	500
12	16	7.06 GeV	441	2.09	500

TABLE II. Zero temperature bottomonium spectroscopy from NRQCD. The $1^3S_1(\Upsilon)$ state is used to set the scale.

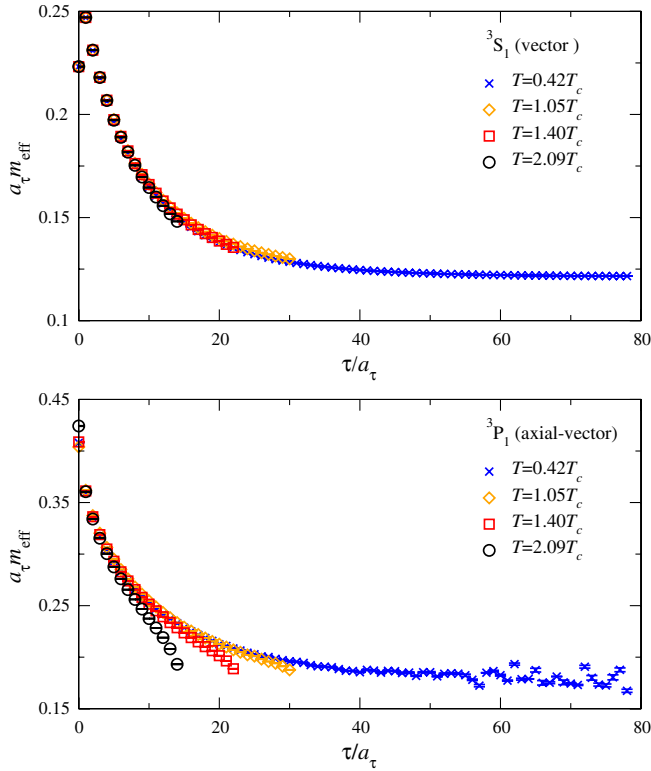| J^{PC}	State	$a_\tau\Delta E$	Mass (MeV)	Exp. (MeV) [34]
0^{-+}	$1^1S_0(\eta_b)$	0.118(1)	9438(7)	9390.9(2.8)
0^{-+}	$2^1S_0(\eta_b[2S])$	0.197(2)	10 009(14)	$\cdots$
1^{--}	$1^3S_1(\Upsilon)$	0.121(1)	9460*	9460.30(26)
1^{--}	$2^3S_1(\Upsilon')$	0.198(2)	10 017(14)	10 023.26(31)
1^{+-}	$1^1P_1(h_b)$	0.178(2)	9872(14)	$\cdots$
0^{++}	$1^3P_0(\chi_{b0})$	0.175(4)	9850(28)	9859.44(42)(31)
1^{++}	$1^3P_1(\chi_{b1})$	0.176(3)	9858(21)	9892.78(26)(31)
2^{++}	$1^3P_2(\chi_{b2})$	0.182(3)	9901(21)	9912.21(26)(31)

FIG. 1 (color online). Effective mass plots in the vector
(above) and axial-vector (below) channel using point sources
for various temperatures: note the different temperature
dependence.

vector channel the data at the higher temperatures do not
show any significant deviation from the low-temperature
result. On the other hand, in the axial-vector channel a
strong temperature dependence is visible, especially at the
two highest temperatures, ruling out pure exponential long
time decay. We take this as a first indication that the Υ is
not sensitive to the quark-gluon plasma up to $T \simeq 2T_c$,
while P waves may melt at much lower temperatures.

To investigate the behavior of P waves in more detail,
we display in Fig. 2 the 0^{++}, 1^{++}, and 2^{++} propagators on
a log-log scale, at the highest temperature. The straight line
is a fit of the form $G(\tau) = c\tau^{-d}$, which is motivated by the
continuum expression in the absence of interactions (4).
We conclude that a power decay describes the data well at
large Euclidean time, with a power $d = 2.605(1)$ which is
close to the continuum noninteracting value of $5/2$.

To visualize the approach to quasifree behavior in an-
other way, we construct effective power plots, using the
definition

$$\gamma_{\mathrm{eff}}(\tau) = -\tau \frac{G'(\tau)}{G(\tau)} = -\tau \frac{G(\tau + a_\tau) - G(\tau - a_\tau)}{2a_\tau G(\tau)}, \quad (6)$$

where the prime denotes the (discretized) derivative. For a
power decay, $G(\tau) \sim \tau^{-\gamma}$, this yields a constant result,
$\gamma_{\mathrm{eff}}(\tau) = \gamma$. On the other hand, for an exponential decay,
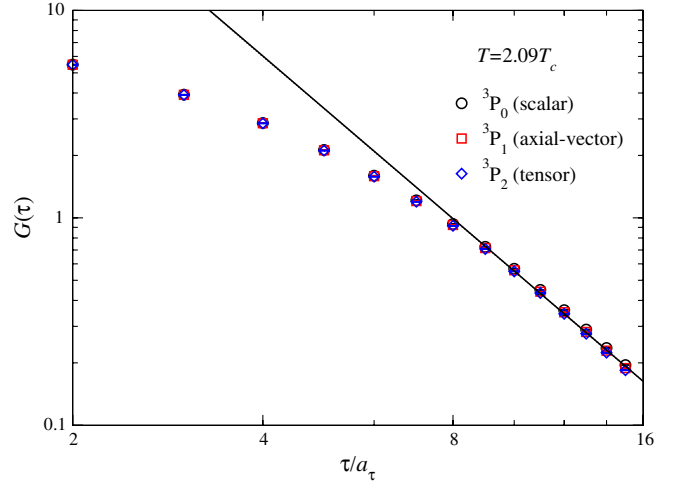

FIG. 2 (color online). P wave propagators on a log-log scale,
at the highest temperature $T = 2.09T_c$. The straight line is a fit to
$G(\tau) = c\tau^{-d}$, with $c = 223.2 \pm 0.5$ and $d = 2.605 \pm 0.001$,
using $\tau/a_\tau = 10, \ldots, 15$.

$G(\tau) \sim \exp(-\Delta E\tau)$, this yields a linearly rising result,
$\gamma_{\mathrm{eff}}(\tau) = \Delta E\tau$. The results are shown in Fig. 3. We con-
firm again that the vector channel displays essentially no
temperature dependence, while in the axial-vector channel
we observe a tendency to flatten out, corresponding to
power decay at large Euclidean time. Also shown are the
effective exponents in the continuum noninteracting limit.
In the axial-vector channel, we observe that the effective
exponent tends towards the noninteracting result at the
highest temperature we consider.

Summary.—We have studied the behavior of S and P
wave bottomonium at high temperature using anisotropic
lattice simulations. The bottom quark is treated via
NRQCD and the light quark dynamics is realized by ex-
ploiting lattice configurations with two flavors of dynami-
cal quarks. The nonrelativistic approximation for the
bottom quark is well justified in the range of temperatures
we have explored, and has many technical advantages. At
nonzero temperature, the main benefit of using NRQCD
over the standard relativistic formulation is that the only
temperature dependence in the NRQCD correlators is due
to the thermal medium, and not due to thermal boundary
conditions. We found that this offers a much cleaner signal
for the crossover between bound and melted states. It also
improves the prospects for extracting spectral functions
inverting Eq. (2) using the maximal entropy method.
This is currently in progress. It will also be interesting to
compare the results presented here with those obtained
using a relativistic treatment of bottom quarks, employing
the same anisotropic action as was used for charmonium
[13,32]. This will give an estimate of the possible system-
atic uncertainties inherent in the two formulations.

Our results indicate that the S wave vector correlator
shows no temperature dependence up to $2.09T_c$, while the
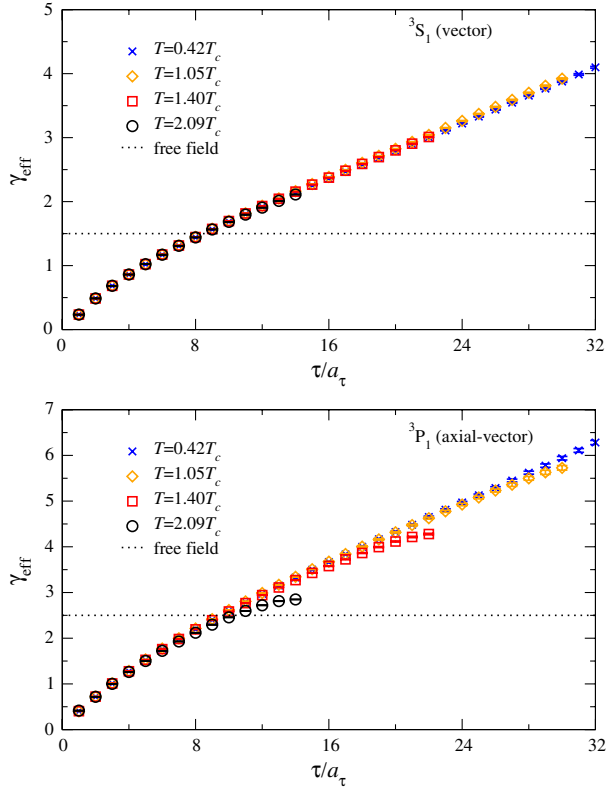P wave correlators are sensitive to the presence of the

PHYSICAL REVIEW LETTERS

FIG. 3 (color online). Effective exponents $\gamma_{\mathrm{eff}}(\tau)$ in the vector (above) and axial-vector (below) channel, as a function of Euclidean time for various temperatures. The dotted line indicates the noninteracting result in the continuum.

thermal medium immediately above T_c. Power-law decay of P wave propagators is visible at $T = 1.4T_c$, while at the highest temperature studied, $T \simeq 2T_c$, we found consistency with nearly free dynamics. The effective power, defined in Eq. (6), is temperature dependent and approaches the noninteracting result at the highest temperature we considered. It would be interesting to understand the temperature dependence and crossover between exponential and power decay analytically, within the framework of effective field theories mentioned above.

[1] T. Matsui and H. Satz, Phys. Lett. B **178**, 416 (1986).
[2] H. Satz, Nucl. Phys. **A783**, 249 (2007).
[3] R. Arnaldi (NA60 Collaboration), Nucl. Phys. **A830**, 345C (2009).
[4] A. Adare *et al.* (PHENIX Collaboration), Phys. Rev. Lett. **101**, 122301 (2008).
[5] R. Rapp, D. Blaschke, and P. Crochet, Prog. Part. Nucl. Phys. **65**, 209 (2010).
[6] B. Alessandro *et al.* (ALICE Collaboration), J. Phys. G **32**, 1295 (2006).
[7] J. P. Lansberg *et al.*, AIP Conf. Proc. **1038**, 15 (2008).
[8] G. P. Lepage *et al.*, Phys. Rev. D **46**, 4052 (1992).
[9] C. T. H. Davies *et al.*, Phys. Rev. D **50**, 6963 (1994).
[10] G. T. Bodwin, E. Braaten, and G. P. Lepage, Phys. Rev. D **51**, 1125 (1995); **55**, 5853(E) (1997).
[11] N. Brambilla, A. Pineda, J. Soto, and A. Vairo, Rev. Mod. Phys. **77**, 1423 (2005).
[12] U. A. Wiedemann, Nucl. Phys. **A830**, 74C (2009).
[13] G. Aarts, C. Allton, M. B. Oktay, M. Peardon, and J. I. Skullerud, Phys. Rev. D **76**, 094513 (2007).
[14] R. Morrin, A. Ó Cais, M. Peardon, S. M. Ryan, and J. I. Skullerud, Phys. Rev. D **74**, 014505 (2006).
[15] A. Jakovác, P. Petreczky, K. Petrov, and A. Velytsky, Phys. Rev. D **75**, 014506 (2007).
[16] P. Petreczky, J. Phys. G **37**, 094009 (2010).
[17] R. Rapp and H. van Hees, *Quark-Gluon Plasma 4*, edited by R. C. Hwa and X. N. Wang (World Scientific, Singapore, 2010), pp. 111–206; see also http://worldsci books.com/physics/7588.html.
[18] J. Fingberg, Phys. Lett. B **424**, 343 (1998).
[19] A. Mócsy and P. Petreczky, Phys. Rev. D **77**, 014501 (2008).
[20] M. Laine, O. Philipsen, P. Romatschke, and M. Tassler, J. High Energy Phys. 03 (2007) 054.
[21] M. Laine, J. High Energy Phys. 05 (2007) 028.
[22] Y. Burnier, M. Laine, and M. Vepsäläinen, J. High Energy Phys. 01 (2008) 043.
[23] A. Beraudo, J. P. Blaizot, and C. Ratti, Nucl. Phys. **A806**, 312 (2008).
[24] N. Brambilla, J. Ghiglieri, A. Vairo, and P. Petreczky, Phys. Rev. D **78**, 014017 (2008).
[25] N. Brambilla, M. A. Escobedo, J. Ghiglieri, J. Soto, and A. Vairo, J. High Energy Phys. 09 (2010) 038.
[26] M. Laine, Nucl. Phys. **A820**, 25C (2009).
[27] A. Beraudo, J. P. Blaizot, P. Faccioli, and G. Garberoglio, Nucl. Phys. **A846**, 104 (2010).
[28] G. Aarts and J. M. Martínez Resco, J. High Energy Phys. 04 (2002) 053.
[29] G. Aarts, C. Allton, J. Foley, S. Hands, and S. Kim, Phys. Rev. Lett. **99**, 022002 (2007).
[30] T. Umeda, Phys. Rev. D **75**, 094502 (2007).
[31] P. Petreczky, Eur. Phys. J. C **62**, 85 (2009).
[32] M. B. Oktay and J. I. Skullerud, arXiv:1005.1209.
[33] C. T. H. Davies *et al.*, Phys. Rev. D **58**, 054505 (1998).
[34] K. Nakamura (Particle Data Group), J. Phys. G **37**, 075021 (2010).